

We are IntechOpen, the world's leading publisher of Open Access books Built by scientists, for scientists

6,900

Open access books available

186,000

International authors and editors

200M

Downloads

Our authors are among the

154

Countries delivered to

TOP 1%

most cited scientists

12.2%

Contributors from top 500 universities



WEB OF SCIENCE™

Selection of our books indexed in the Book Citation Index
in Web of Science™ Core Collection (BKCI)

Interested in publishing with us?
Contact book.department@intechopen.com

Numbers displayed above are based on latest data collected.
For more information visit www.intechopen.com



Marine-Based Carbon and Silicon Carbide Scaffolds with Patterned Surface for Tissue Engineering Applications

Miriam López-Álvarez, Julia Serra,
Alejandro de Carlos and Pío González
*University of Vigo
Spain*

1. Introduction

This chapter deals with the development of bioinspired biomaterials based on carbon and silicon carbide (SiC) both derived from marine resources, specifically, from the sea rush *Juncus maritimus* Linnaeus. These three dimensional scaffolds with interconnected hierarchical porosity and a patterned surface, both preserved from the natural plant of origin, constitute a promising approach for tissue engineering.

In the last decade, a broad range of solutions have been developed for each particular function in tissue regeneration, as devices with high mechanical stability for large bone defects in load-bearing long bones or injectable materials for craniofacial surgery. The fabrication of patterned surfaces on biomaterials, especially focused on parallel channels, is another of the proposed solutions that is having a increasing interest in the last years. The need to promote an oriented growth of bone tissue, which presents in long bones, an aligned orientation of calcium phosphate crystals is one of the potential applications thought for these patterned surfaces. Thus, this oriented growth of osteoblasts will provide a bridge for bone regeneration in disrupted areas in order to correct defects in this type of bones and will improve the distribution of forces in load-bearing implants by guiding the growth of bone tissue in certain areas or in certain directions (Wiemann et al., 2007; Wise et al., 2008).

Different materials such as hydroxyapatite, silicon, polystyrene, polycaprolactone, etc. have been patterned for the same purpose using laser techniques, electrospinning or others, resulting in expensive processing protocols (Wise et al., 2008). Cells and extracellular matrix (ECM) fibrils in most natural tissues are not random, but exhibit well-defined patterns and specific spatial orientation. The variability in dimensions and distribution of channels on the patterned surfaces to mimic the natural biostructures that have, furthermore, a network of micro and nanoscale pores and channels, is required to optimize the flow of the cell growth medium, products of metabolism and waste. This is extremely difficult and very expensive to replicate artificially (Green et al., 2003; Huebsch & Mooney, 2009; Lakes, 1993) and has led to the inspiration in nature, where structures with a complex and hierarchical organization abound. Thus, the biodiversity that characterizes the marine environment represents an enormous potential for the acquisition of novel microstructures.

The use of biostructures derived from the marine environment for their application as biomaterials is very recent. For instance, several authors have proposed in the last years, the use of different marine species like coral skeletons, sea urchins and sponges as three-dimensional biomatrices (Abramovitch et al., 2006; Green et al., 2008, Cunningham et al., 2009). The results have confirmed that the three dimensional topography and the surface parameters of these materials influence positively in the cell differentiation. Topography and composition of the material have been proven to affect cellular functions, such as adhesion, growth, motility, secretion and apoptosis.

Apart from the patterning, scaffolds should have an internal structure designed with a predetermined density, pore shape, and size, with appropriate interconnection pathways. High porosity levels are necessary to support migration and proliferation of osteoblasts and mesenchymal cells, bone tissue ingrowth, vascular invasion, nutrient delivery, and matrix deposition in empty spaces. In fact, the main critical factor affecting bone formation is the presence of a combined macro- and microporosity, since macropores (size $>100\ \mu\text{m}$) have a critical impact on osteogenic outcomes, promotion of vascularization, and mass transportation of nutrients and waste products (Wang et al., 2000), while micropores (size around $10\ \mu\text{m}$) favor capillary formation. Currently, it is commonly accepted that 3D scaffolds should also contain nanoporosity to allow diffusion of molecules for nutrition and signaling (Ratner, 2004). Pore interconnection also plays a key role in the overall biological system, since it provides the channel for cell distribution and migration, allowing efficient *in vivo* blood vessel formation. Furthermore, pore wall roughness contributes to increase the surface area, protein adsorption, and ion exchange (Yang et al., 2008; Bettinger et al., 2008).

Following these considerations, open structure-based scaffolds with appropriate pore size, interconnectivity, and total porosity should be modeled and developed in order to provide *in vivo* blood vessel invasion and neobone tissue ingrowth within the scaffolds. The proposed sea rush *Juncus maritimus* Linnaeus has a vascular system uniformly distributed throughout its section that provides a hierarchical interconnected porosity, with channels distributed along the entire plant. As an added value, this plant presents a surface patterning in the upper epidermal layers with channels aligned in the direction of the plant's growth (Dawes, 1998).

The particular motivation for this work was to engineer two different porous scaffolds of carbon and silicon carbide with a patterned surface. Both materials have been already proven as biocompatible. The use of carbon in the biomedical industry dates back to the late sixties when the unique blood compatibility of pyrolytic carbon as well as its physical and mechanical properties allowed, since 1968, its use in heart valve components (DeBaakey-Surgitool). This material has also been applied as a coating on vascular grafts and recently, carbon has experienced an increasing interest in the form of nanotubes and nanofibers (Gómez et al., 2007; Harrison & Atala, 2007). The application of silicon carbide obtained from wood precursors in the biomaterials field derived from its potential to exceed the demand in orthopedic materials due to its inherent characteristic of being chemically inert and therefore resistant to aggressive chemical and mechanical environments, also with the interconnected and hierarchical porosity preserved from the plant vascular system (Borrajó, 2006). Several *in vitro* studies have demonstrated its biocompatibility with excellent results in proliferation and osteoblastic activity with different cell lines, as well as *in vivo* tests with implants in femur of rabbit where it has been shown penetration of bone tissue into the porous structure of the bio-inspired silicon carbide (de Carlos et al., 2006; López-Álvarez et al., 2010; González et al., 2009).

2. Scaffolds fabrication

Several techniques can be followed for the fabrication of ceramics. More specifically, for the silicon carbide obtaining, the sintering with or without applying pressure over silicon carbide powder and carbon, the chemical vapour deposition (CVD) by a gas containing carbon and silicon, or the compacted by reaction over carbon and silicon carbide particles, are the most commonly used. Other technique, the fabrication by pyrolysis and reactive infiltration with molten silicon from plant precursors, is the selected in this work. This one implies lower processing temperatures than in the sintering protocols, the substitution of silicon carbide powder by silicon powder and the plant precursor, both cheaper and higher velocity of fabrication than in the protocols with gas reactions as in chemical vapour deposition (Borrajo, 2006).

Thus, the bio-inspired carbon scaffolds obtained from the sea rush *Juncus maritimus* Linnaeus were fabricated by submitting the plant to air drying for several days and then introduced in a pyrolysis furnace inside an alumina melting pot. The pyrolysis process consisted in the thermal decomposition of the plant precursor (Maity et al., 2010; Singh et al., 2003; Varela-Feria et al., 2002) by a gradual increase in temperature of 2°C/min up to 500°C. The furnace was then maintained at that temperature for 10 minutes, followed by a gradual decrease of 20°C/min down to room temperature. This process was followed for the conversion of the structural carbon in the form of cellulose in the plant into solid carbon. Once obtained the carbon scaffolds, due to its marine origin, the removal of salts (sodium chloride and potassium chloride) was seen as necessary. Samples were subjected to ultrasonic baths of 60 minutes with warm milli-Q water.

According to the literature (Tang & Bacon, 1964) and under the hypothesis of low heating slopes (2°C/min in our case) this process is explained by four phases. The first one is the evaporation of absorbed water at 150°C. This water loss leads to the second phase, the breaking of the structure of cellulose between 150 and 240°C. The third one is the decomposition of organic polymers, mainly hemicellulose, due to the breaking of C-C and C-O bonds between 240 and 400°C, resulting in the release of carbon monoxide, carbon dioxide and water. Finally, the decomposition of cellulose and lignin at a high rate from 290°C until 400°C and more slowly up to the final 500°C, takes place. Therefore, it is at a temperature higher than 400°C that the induced thermal decomposition is accompanied by the restructuring of the carbon atoms, releasing residual hydrogen and eliminating defects, causing an increase in the degree of crystallinity (Tang & Bacon, 1964; Borrajo, 2006; Byrne & Nagle, 1997). However, Pappacena *et al.* (Pappacena et al., 2009) demonstrated recently that after subjecting wood to a one hour pyrolysis process with temperatures between 400 and 2500°C, the obtained carbon is always turbostratic and not graphite even if higher temperatures tend to slightly increase the degree of crystallinity.

To obtain the bio-inspired silicon carbide scaffolds, the carbon scaffolds were covered by the optimized amount of pure silicon powder and infiltrated, under vacuum conditions, at 1550°C during 30 minutes. Silicon melting point was exceeded (1410°C) and let it flow through the interconnected porosity reacting with carbon. That temperature was achieved by following a gradual heating ramp of 10°C/min up to 1200°C and of 5°C/min from 1200 to 1550°C. After the 30 minutes of permanence the furnace temperature was decreased by a well-controlled ramp of 10°C/min to room temperature and the silicon carbide (SiC) ceramics were obtained. It has been proven in the literature that the final structure of SiC depends on the temperature achieved, obtaining the form β -SiC at temperatures around

1550°C, while hexagonal polytypes (α -SiC) are obtained at 2200-2500°C (Dressler & Riedel, 1997).

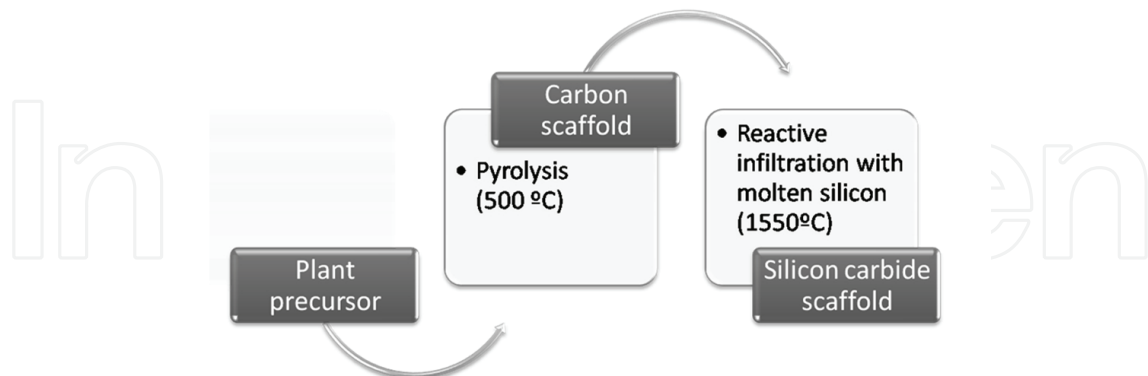


Fig. 1. Diagram of the fabrication process

Carbon graphite structure and β -SiC cubic poly-type are represented in Figure 2 (a) and (b) respectively.

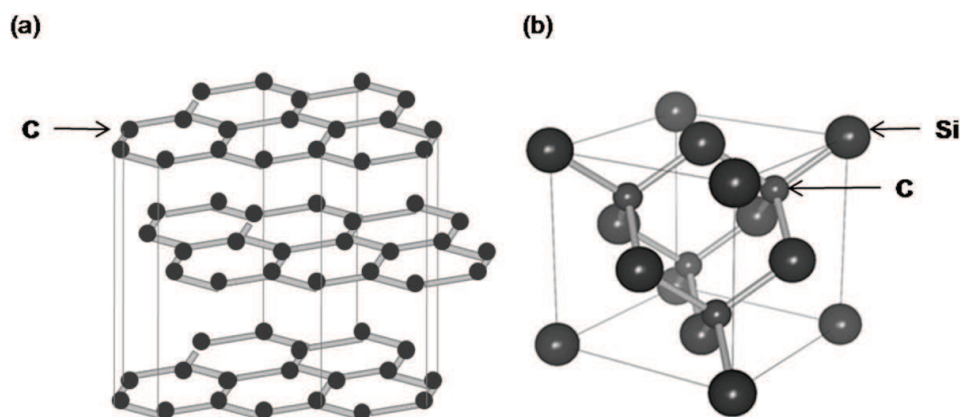


Fig. 2. Chemical structure of graphite (a) and β -SiC (b).

3. Physicochemical properties

Different techniques based on the interaction between a visible light beam (optical microscopy and Interferometric profilometry), high energy beam of electrons (SEM), X-ray beam (EDS/XRF/XRD) or a infrared radiation source (FTIR) and the atoms that constitute the material permit the evaluation of its morphology and chemical composition. At the same time the mercury's strong surface tension prevents its penetration into a porous material by capillarity so that it is used to measure the pore distribution in the sample by applying pressure (mercury porosimetry) (Ishizaki et al., 1998).

The morphology of the marine plant *Juncus maritimus* presents in cross section the vascular bundles with pores of 20-25 μm that correspond to the xylem and of < 5 μm which are the phloem, and both of them distributed through the whole section of the plant communicating the central section with the most external layer of the epidermis of the plant (Figure 3 (a)). Therefore, abundant porosity with variable pore sized and homogeneously distributed and

interconnected with the epidermis and between them guaranteed by the vascular system constituents is presented in this marine plant. At the same time, the surface of this sea rush presents a macro-patterning with channels of around $100\ \mu\text{m}$ in width oriented in the plant's growth direction and, within each macrochannel, a micro-patterning with channels of around $7\ \mu\text{m}$ oriented in the same direction (Figures 3 (b) to (d)). Arranged in rows on both sides of the macrochannels are the stomata, which correspond to oval-shaped pores used by the plant to regulate the gas exchange and water loss (Dawes, 1998), with a size of around $30\ \mu\text{m}$ in diameter (Figure 3 (c)).

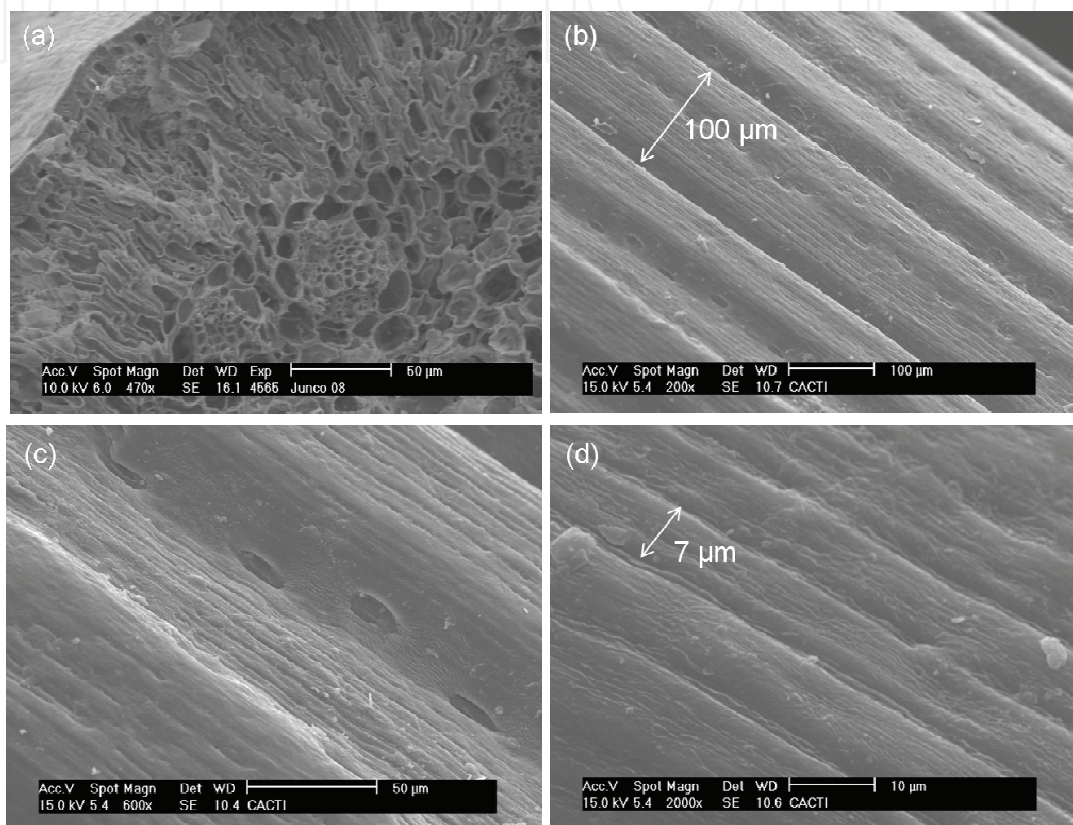


Fig. 3. SEM images of the sea rush *Juncus maritimus* in cross section (a) and surface patterning (b-d).

The carbon scaffold obtained from this sea rush preserved the double patterning with the macro and microchannels and the stomata observed previously in the natural plant as shown in Figure 4 (a). On the other hand, the silicon carbide scaffold showed the preservation of the natural microstructure after the ceramics processing, especially the macropatterning together with an increase at the surface roughness along the channels, mitigating the micro-channels topography, as consequence of the silicon carbide crystals formed on them (Figure 4 (b)). In both micrographs a detail at higher magnification ($\times 4000$) of each surface is shown, it is particularly interesting the β -SiC cubic poly-type crystal image in the Figure 4 (b). Three-dimensional images of the patterned surfaces of both materials obtained by interferometric profilometry showed by representing the variations in profile with blue for lower regions and red for the higher ones, the macro-pattern with parallel channels distributed along the surface in both materials (Figures 4 (c) and (d)). Profile variations along the channels in the silicon carbide surface as consequence of the SiC crystals

can be observed in Figure 4 (d). When compared both surfaces in terms of the arithmetic average of the roughness profile (Ra), the values were 1.6 μm for the carbon and 3.5 μm for the silicon carbide pieces.

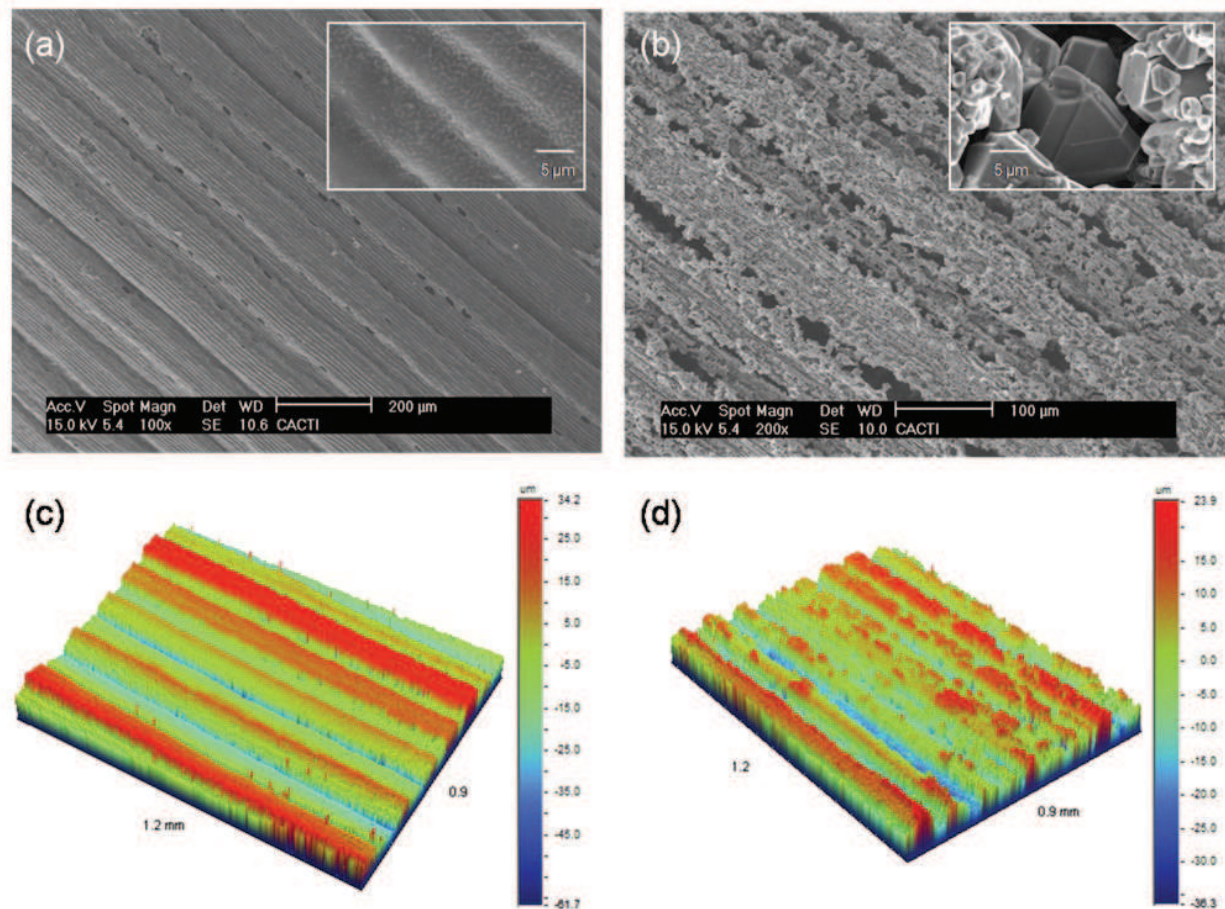


Fig. 4. SEM (a, b) and interferometric profilometry images (c, d) of a carbon scaffold (a, c) and a silicon carbide scaffold (b, d) both obtained from the sea rush *Juncus maritimus*.

The XRF analysis reveals that the composition of the C scaffold is of carbon in a percentage of 95.98% of the total mass (Table 1). Values of around 1% oxygen and sodium were detected, with close percentages of chlorine and potassium. Phosphorus and magnesium were also detected in concentrations of 0.241 and 0.150%, respectively. Calcium, sulfur, silicon and aluminum were detected in trace amounts (<0.01%). The SiC scaffold has a percentage in silicon of 69.64% and in carbon of 29.78%. In the remaining 0.58%, the most abundant element is oxygen and aluminum (1-0.1%) followed by, iron, calcium, chlorine, potassium, titanium, sulfur (0.1-0.01%) and, in trace concentrations (<0.01%), magnesium, nickel and zinc.

The presence of carbon in both materials comes from the natural plant, where the majority of the elemental composition is attributed to C, H and O, elements that can correspond to both structural compounds such as cellulose and lignin and other non structural organic matter (C-C, C-H, O, N, S, P, halogens...) in a total percentage of 93.958%. Chlorine, potassium and sodium are easily attributed to the most abundant sea salts, sodium chloride and potassium chloride, present in the natural plant in a percentage >1% for chlorine and

potassium and in the range 1-0.1% for sodium. Phosphates and silicates are nutrients found in the marine environment. Regarding the presence of zinc, this element is a micronutrient in the plant included in the structure of several enzymes what leads to attribute its presence to its own metabolism but, at the same time, the ability of this marsh plant to accumulate trace metals found in the sediment (bioaccumulation), such as cadmium, copper and zinc (Almeida et al., 2006), has been proven. The presence of aluminum is away from expected composition in this specie and can only be explained by its incorporation from the collection area. It should be noted the total absence of nitrogen that could be explained by one of the ecological requirements of this plant, a nitrogen-poor soil.

The comparison with the natural sample shows that the composition of the C scaffold has been greatly enriched in carbon with the removal of organic matter, while the presence of chlorine and potassium has been significantly decreased after subjecting the samples to several ultrasonic washes. Calcium, sulfur, silicon and aluminum were also considerably reduced and the presence of iron, zinc and nickel was no longer detected. In the case of SiC it was reduced the percentage of all elements, except silicon and it was detected the titanium for the first time. The presence of oxygen confirmed the formation of oxides with silicon or other elements. The composition of the SiC scaffold with oxides of different elements in smaller concentrations supposes a closer approximation to the living tissue composition, where the traces constituents are proven to benefit the cellular activity (Cousins, 1995).

(%)	C	H	O	Cl	K	Na	Si	Al	S	Ca	Fe	P	Mg	Ti	Ni	Zn
Natural	37.98	3.188	52.79	1.710	1.790	0.400	0.606	0.220	0.190	0.490	0.130	0.100	0.084		0.098	0.220
Cscaf.	95.98		1.091	0.833	0.603	1.010	0.065	0.008	0.073	0.042		0.241	0.150			
SiCscaf.	29.78		0.216	0.038	0.015		69.64	0.130	0.014	0.052	0.091		0.007	0.016	0.003	0.003

Table 1. Elemental composition of the natural plant, carbon and silicon carbide scaffolds measured by XRF.

Both materials were analyzed by FT-IR (Figure 5). The main IR absorption bands can be attributed to the following functional groups (Smith, 1999; Dragnea et al., 2001; Qian & Jin, 2006): C-H groups exhibit sharp peaks located between 2800 and 2960 cm^{-1} associated to C-H₂ symmetric stretching (2860-2875 cm^{-1}), C-H₂ asymmetric stretching (2910-2930 cm^{-1}) and C-H₃ symmetric stretching (2950-2960 cm^{-1}). Moreover, well resolved peaks attributed to C-H₃ symmetric and asymmetric bending modes emerge at around 1380 and 1436 cm^{-1} , respectively. Carbonate groups can be identified by two absorption bands; the peak around 877 cm^{-1} associated to C-O bending vibration out-of-plane and 750 cm^{-1} related to C-O bending vibration in-plane. Other band at 1568 cm^{-1} can be associated to C=O stretching mode corresponding to carboxyle groups. The broad absorption band of absorbed water can be observed in the range 3200-3700 cm^{-1} (water stretching vibration). The hydroxyl group (-OH) has a stretching vibrational mode that appears at around 3571 cm^{-1} with a shoulder at 3550 cm^{-1} . In the case of the IR analysis of SiC scaffolds (Figure 5(b)) and besides of the previous described bands, new absorption peaks can be identified; SiC groups around 782 and 798 cm^{-1} associated to Si-C stretching vibration mode and Si-O groups which exhibit bands located around 1100 cm^{-1} , 800 cm^{-1} and 450 cm^{-1} identified as symmetric stretching, bending and rocking vibration modes respectively.

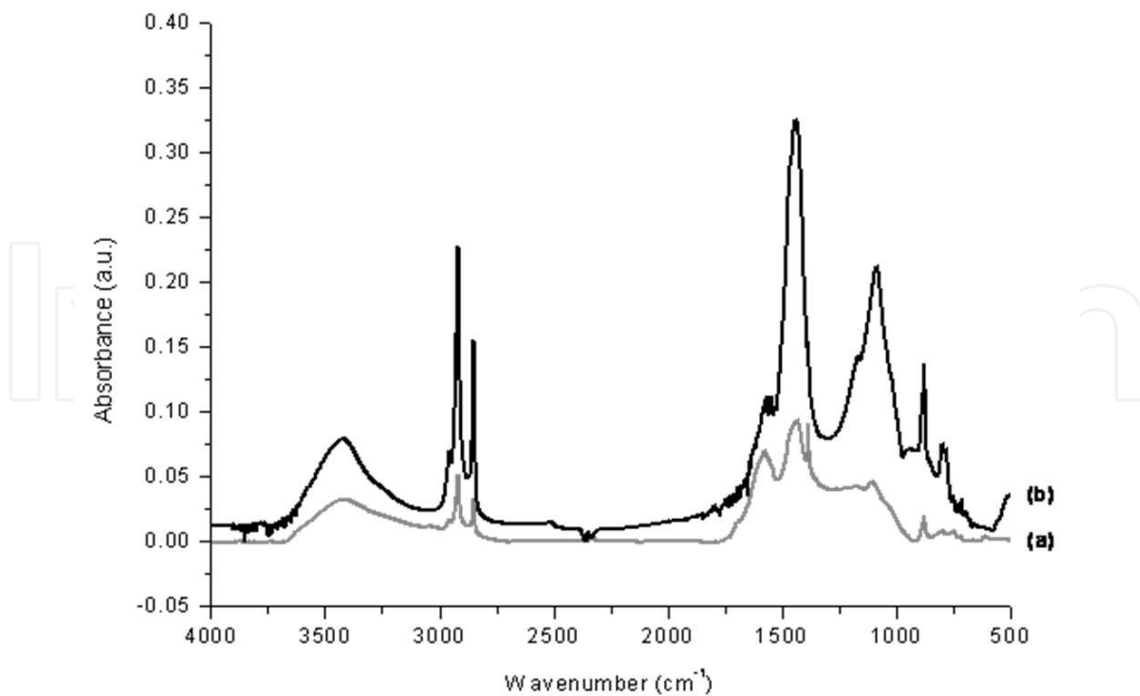


Fig. 5. FTIR analysis of the carbon (a) and silicon carbide scaffolds (b).

Two different three-dimensional scaffolds are presented in this chapter with different compositions but both made from the same natural plant precursor by following a relatively simple manufacturing process. A scaffold per se implies a porous matrix designed to guide the cells growth and to permit their ingrowth inside the matrix to favor the integration of the new tissue formed and also its vascularization. In both scaffolds the porosity of the original sea rush *Juncus maritimus* was preserved. However and due to the different chemical structure of materials, scaffolds obtained differ in size and total percentage of pores. The distribution of pores in the carbon scaffold (Figure 6) was measured, presenting a percentage of total porosity estimated in a 63% with nanopores (0.03-0.2 μm in diameter), mesopores (1-10 μm) and macropores (80-150 μm). Silicon carbide scaffolds presented a double size-scaled porosity with mesopores between 1 and 50 μm of diameter and macropores between 80 and 150 μm and a percentage of total porosity of 48%. After the infiltration with molten silicon in the ceramics processing, obviously, the nanoscaled pores were clogged.

When gone in depth into the porous structures found in the human tissues, a great variety was found even in the same type of tissue as, for instance, bone where the total percentage of pores per volume varies from 50 to 90% in femoral trabecular bone and between 3 to 12% in the cortical bone of the tibia. The same variety was observed in terms of pores sizes where two requirements have been stated as the necessity of pores larger than 100 μm to favor the formation of bone tissue with high vascularity and oxygenation, and also pores with diameters in the mesoscale (1-50 μm) or even nanoscale (<1 μm) due to the recent results that indicate the higher adsorption of proteins for the anchorage of the cells when these small pores are present (Karageorgiou & Kaplan, 2005). Both scaffolds satisfy this hierarchical requirement, being a priori more beneficial for tissue engineering the carbon scaffold respect to the silicon carbide because of the nanopores presence.

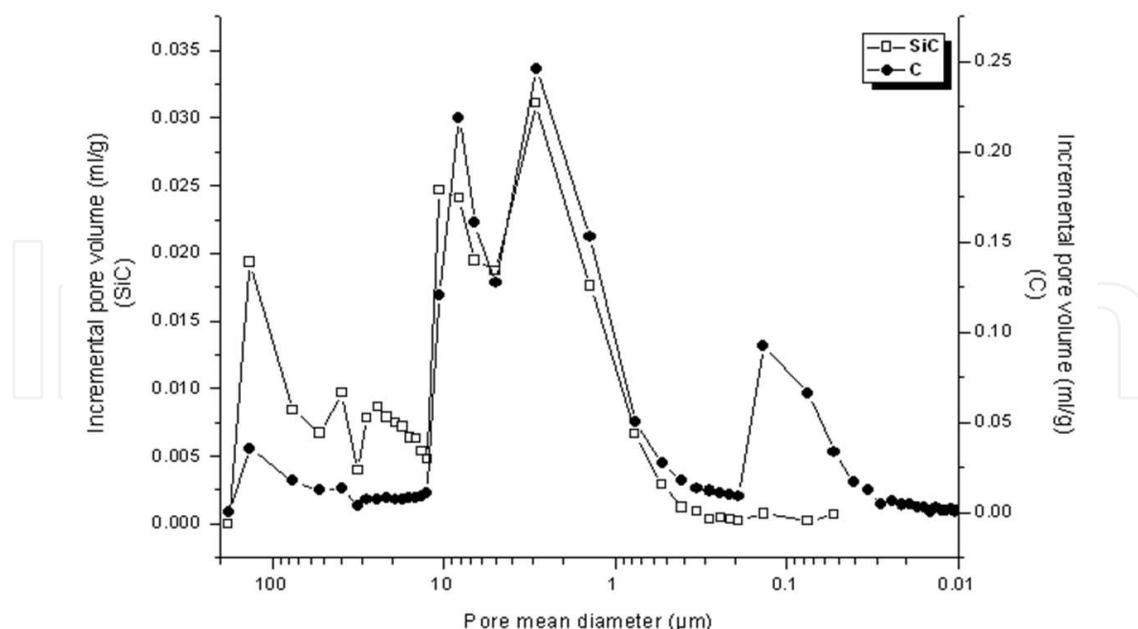


Fig. 6. Pore size distribution obtained by mercury porosimetry of a carbon scaffold (black point) and a silicon carbide scaffold (white square).

4. Evaluation of the cell morphology

The first step in the evaluation of a material as biocompatible is the cell morphology study. For testing the cell proliferation and alignment on the bio-inspired carbon and silicon carbide scaffolds proposed, pre-osteoblasts from the cell line MC3T3-E1 (ECACC, UK) were selected. This cell line was established from explants of mouse calvaria and it is considered as a standard model for *in vitro* testing of osteogenesis. In defined conditions of culture these cells differentiate to osteoblasts with the production of mature extracellular matrix and its mineralization (Wang et al., 1999; Raouf & Seth, 2000). The alignment of this cell line once differentiated to osteoblasts has been previously confirmed on different microgrooved substrata (Wang et al., 2000). Finally, and unlike other cell lines such as Saos-2 or MG-63, the selected cell line was not derived from osteosarcoma what implies a more adjusted to reality behavior. Cells alignment and proliferation on both carbon and silicon carbide scaffolds were analyzed by scanning electron microscopy.

As it is shown in the SEM micrographs of both surfaces (Figure 7), pre-osteoblasts grew aligned on both surfaces after 6 hours of incubation, by extending their filopodia along the plant-derived pattern. Cells clearly proliferated following the orientation marked by the channels, in addition, it can be appreciated how, after making contact with the surface of the material, the cells reoriented their filopodia in the marked direction (see white arrows Figure 7 (a)). Thus, the surface patterning promoted the alignment of pre-osteoblasts.

Once confirmed the cell alignment at short term, the seeded scaffolds were analyzed after longer periods of incubation with the pre-osteoblasts. Figure 8 presents both scaffolds after 7 days of incubation. On the patterned surfaces of both materials (a) and (c) it can be observed that cells have covered the whole macro-channeled surface and began to fill the spaces between. The cells present healthy appearance, with the characteristic flat morphology, adapting perfectly to the surface so that the micro-patterning underneath in the carbon scaffold (a) and the crystalline morphology underneath in the silicon carbide (c) can be still

distinguished. As a porous and three-dimensional scaffold it was also important to evaluate the cell morphology in the cross section of the piece, where the porous structure is prevalent and the patterning is absent. As it can be observed in images (b) and (d) both sections have been also covered by the cells that grew appropriately inside the pores covering the cross sections, without a determined orientation due to the patterning absence.

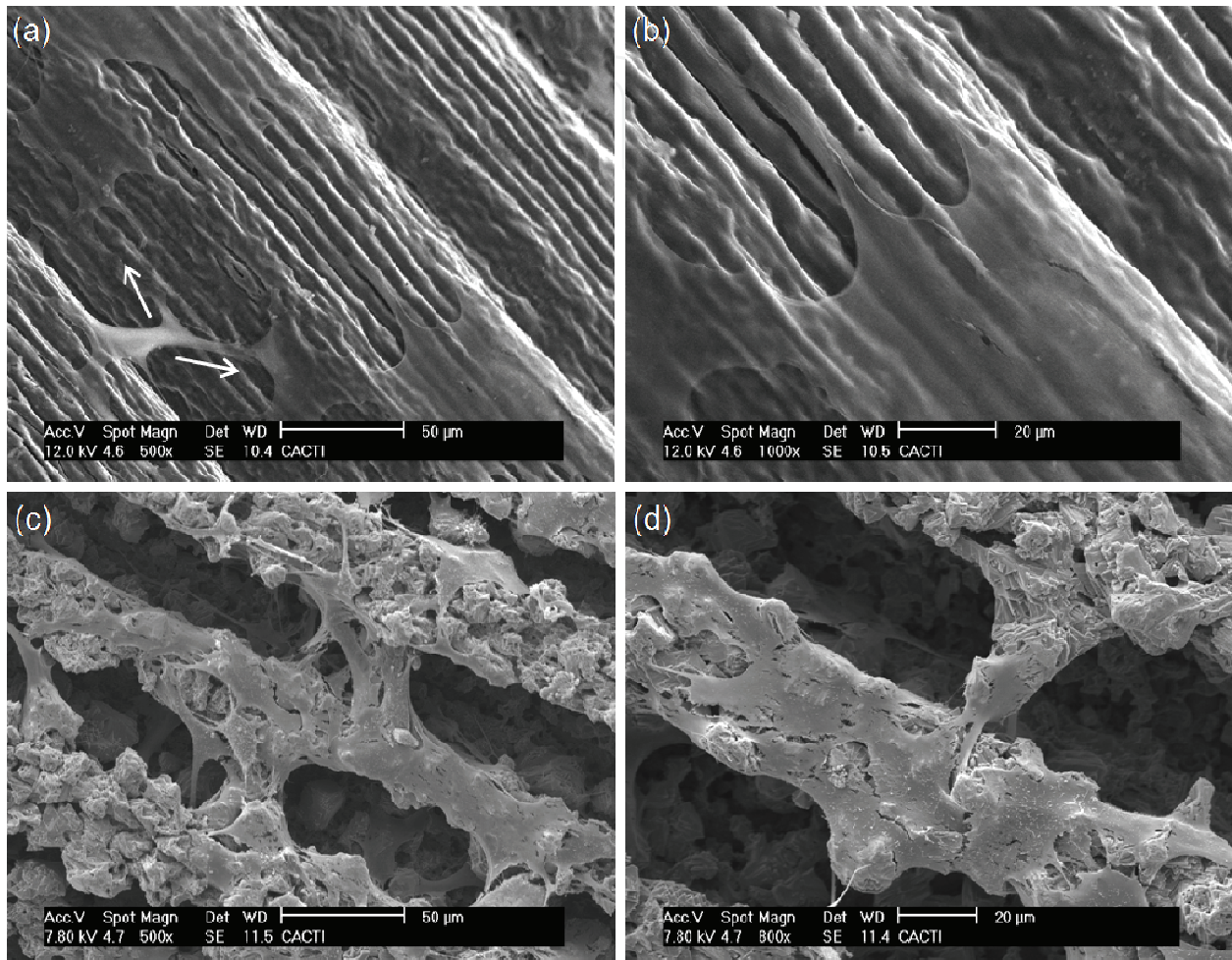


Fig. 7. SEM images showing the morphology of MC3T3-E1 cells on the patterned surface of a carbon scaffold (a, b) and a silicon carbide (c, d) after 6 hours of incubation.

The SEM micrographs of the carbon and SiC scaffolds after 28 days of incubation showed the surface completely covered by a thick layer of cells. However, in both cases the macro-patterning of the pieces was still clearly visible (a) and (c). Although after 28 days of incubation, the cells grow on a layer of cells and not directly on the surface structure of ceramics, it appears that they proliferate with a preferred orientation in the direction marked by the structure of both materials.

5. Evaluation of the cell differentiation

The evaluation of the differentiation of cells to osteoblasts is required as a proof of their functionality and of the suitability of the material. One of the most widely used tests consists on the measure of the activity of alkaline phosphatase. Alkaline phosphatase is an enzyme

responsible for removing phosphate groups of various types of molecules in an alkaline environment. It is found in almost all body tissues, but its presence is particularly high in bone, and its expression, characteristic of early differentiation of osteoblast cells.

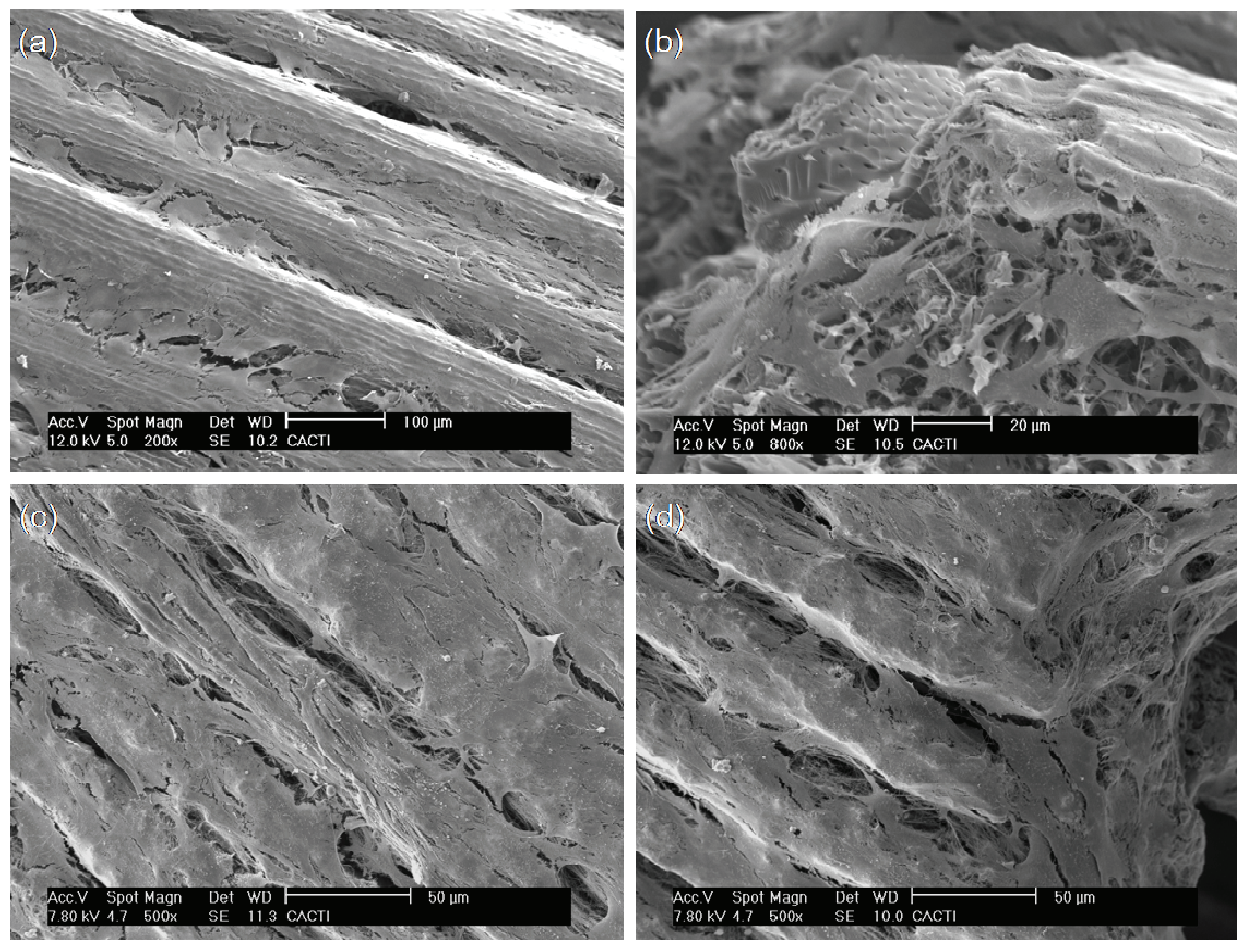


Fig. 8. SEM images showing the morphology of MC3T3-E1 cells on the carbon piece at patterned surface (a) and at the end of the scaffold in transversal section (b) and on the silicon carbide at the patterned surface (c) and at the end of the scaffold in transversal section (d) after 7 days of incubation.

To quantify osteoblastic activity and therefore evaluate the differentiation of MC3T3-E1 cells to osteoblasts enzyme activity of alkaline phosphatase (ALP) was measured. ALP activity on carbon and silicon carbide was evaluated over time (1, 7, 14, 21 and 28 days) using tissue culture polystyrene (TCP) as reference material (Figure 10). The enzyme activity estimated on carbon appeared with low values after 1 and 7 days of incubation followed by a dramatic increase on day 14th and continuing to increase until day 28 of culture. The sharp increase at day 14th suggested that the cells began to differentiate in that period. In the case of SiC the pattern followed is the same but with a much less marked increase on day 14th, to increase on day 21 and keeping up on day 28, but always in activity values lower than carbon (about 30% lower). The results for the reference material (TCP) followed the pattern found in the literature and validated the experiment. The statistical analysis of the data revealed a significant difference ($p < 0.05$) between alkaline phosphatase activity on C and TCP synthesized after 21 days of culture and SiC and TCP at 1 and 21 days of incubation ($p < 0.01$), and 28 days ($p < 0.05$).

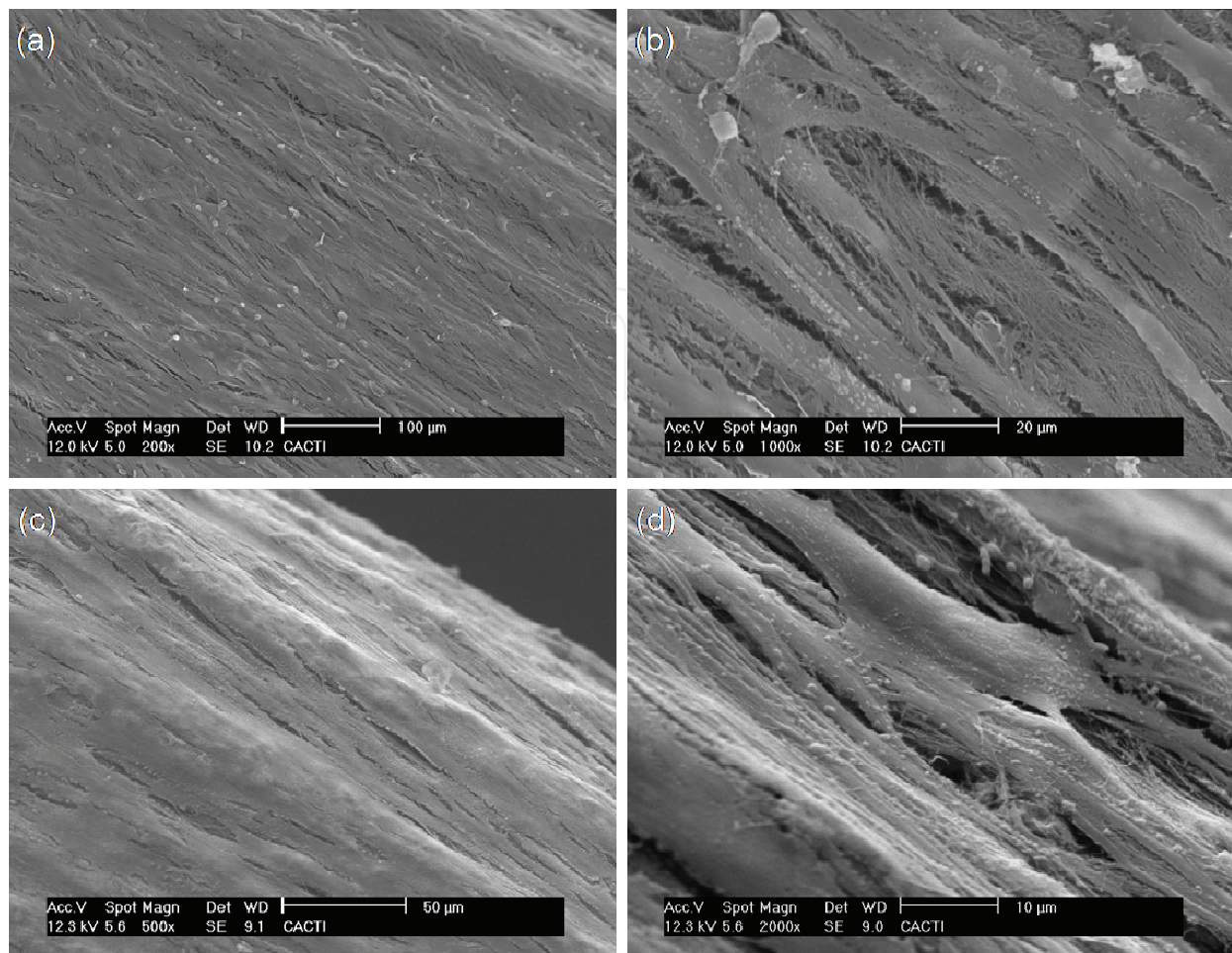


Fig. 9. SEM images showing the morphology of MC3T3-E1 cells on the patterned surface of a carbon scaffold (a, b) and of a silicon carbide scaffold (c, d), after 28 days of incubation.

Once differentiated to osteoblasts, cells appeared immersed in a complex network of fibers producing the extracellular matrix, oriented in all directions, as seen clearly in Figure 11 (a) corresponding to the surface layer of cells after 28 days in the carbon scaffold. These fibers can be appreciated in more detail in the micrograph (b). Taking into account the incubation period and the evident differentiation stage, these fibers could correspond to collagen. To confirm that, a striation across the fiber and through the whole one, should be distinguished. It can be detected a slightly striation along them (see arrow) however, this is mitigated by the gold coating of the SEM sample preparation. Regarding the silicon carbide surface after 28 days of incubation it can be observed how the cells start to secrete extracellular matrix including complex networks of filaments (c) and (d).

As it is well known bone tissue is constituted by the presence of an organic part, with the synthesis of extracellular matrix (collagen fibers) and a mineral part, production of calcium phosphate. EDS analysis can be used to reveal the presence of calcium phosphate deposits. Thus, the surface of the cell layer after 28 days of incubation on both C and SiC scaffolds was analyzed and the EDS spectra are represented in Figure 12. The presence of calcium was confirmed in several zones of the C scaffolds (Figure 12 (a, b)) and totally absent in the SiC scaffolds (Figure 12 (c)). The calcium presence can correspond to the mineralized extracellular matrix by the differentiated MC3T3-E1 pre-osteoblasts.

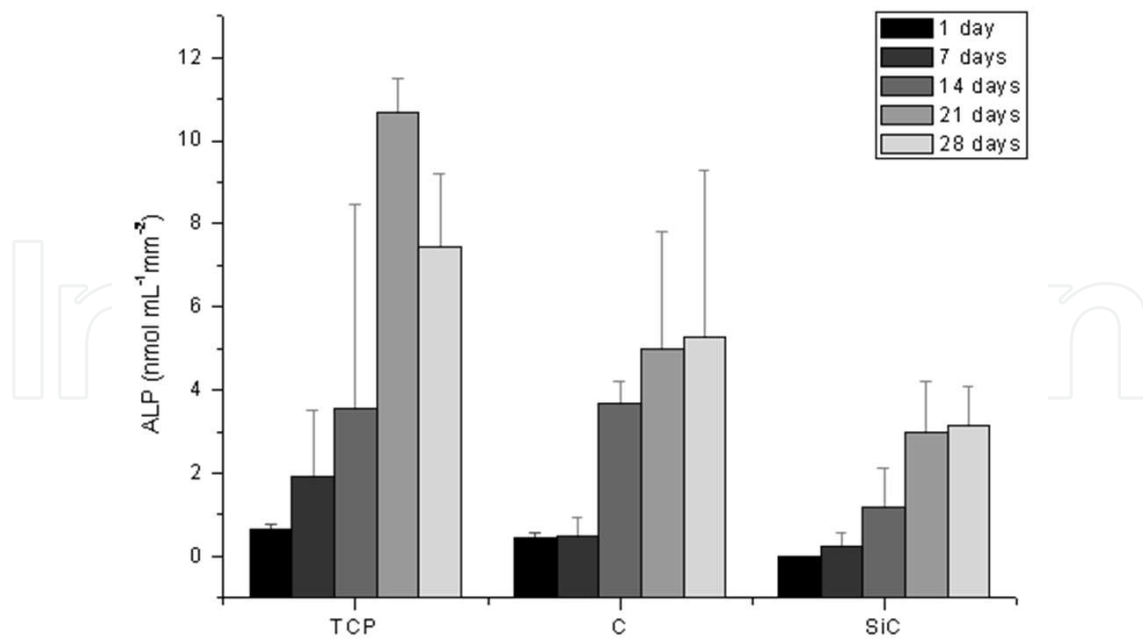


Fig. 10. ALP activity on C and SiC scaffolds after 1, 7, 14, 21 and 28 days of incubation.

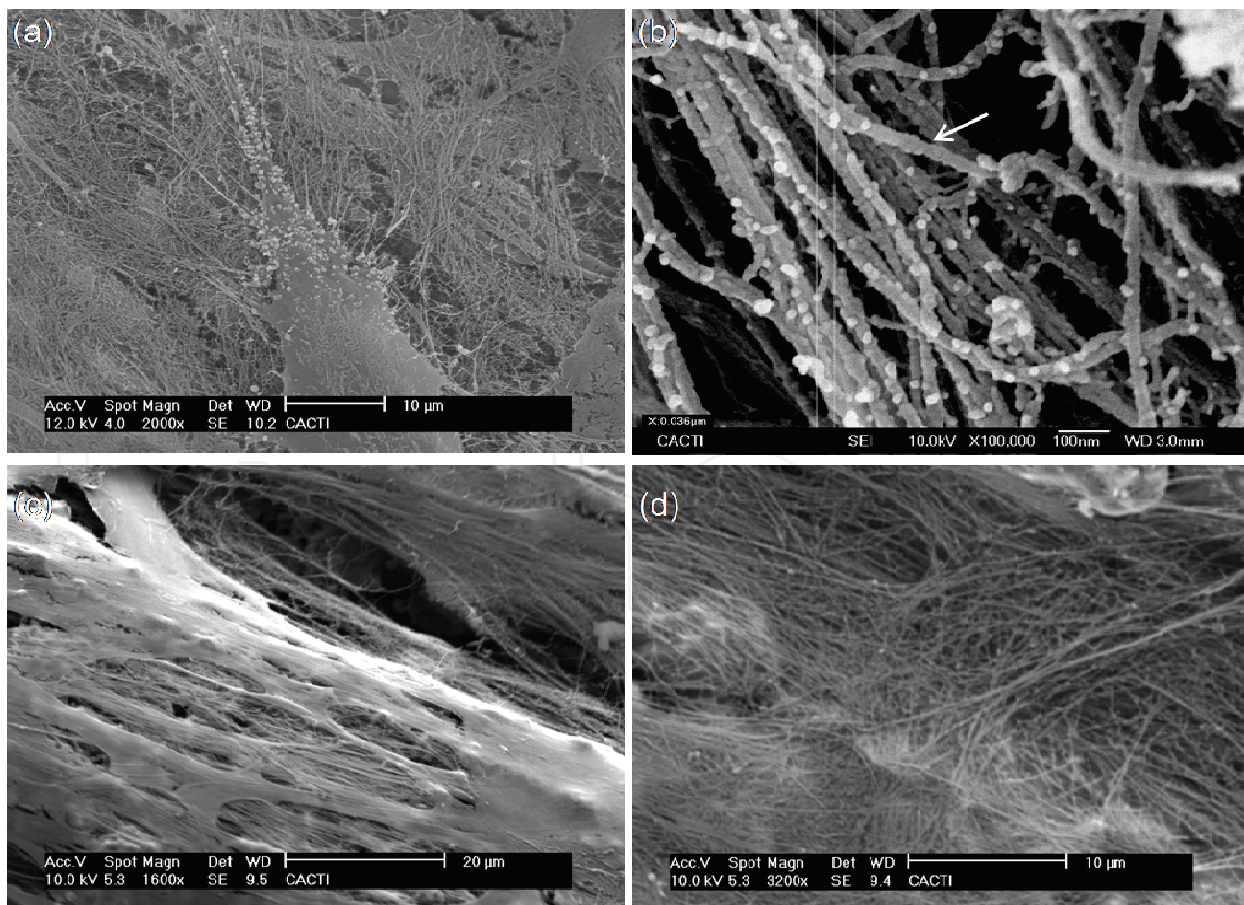


Fig. 11. SEM micrographs of the cell layer after 28 days on the surface of carbon (a, b) and silicon carbide (c, d).

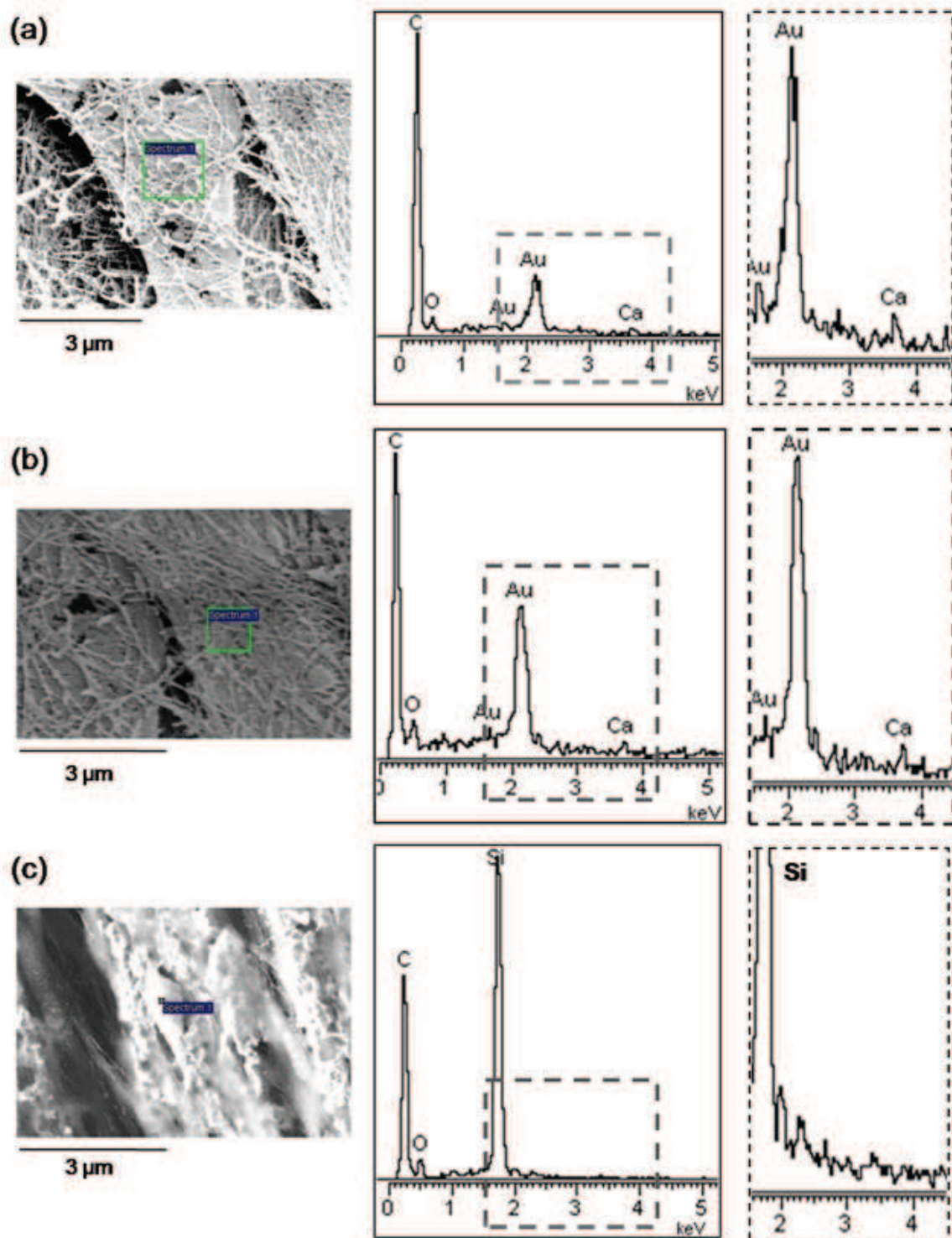


Fig. 12. EDS spectra of the carbon (a, b) and silicon carbide (c) cell layer after 28 days of incubation with MC3T3-E1. The site of interest analyzed, the general spectra and a magnification at the calcium peak area of 84 counts are represented for each one. The presence of gold comes from the SEM sample preparation

Apart from being attributed to the cells, the calcium presence at the carbon scaffolds could be assigned to the composition of the material itself (since that it could be possible that the

electron beam has penetrated deeper in the monolayer of the cells achieving the material) or to the contributions of the culture medium of cells (MEM-alpha) that was renewed every two days during culture. After 28 days the quantity of calcium deposited could be higher enough to be detected by the EDS. Attending to the elemental composition (Table 1) calcium was detected in the carbon scaffold in a percentage of 0.042% and in the silicon carbide the percentage was similar (0.052%). The non-detection of calcium in the silicon carbide cell monolayer discarded the first possibility related to the material composition. Regarding with the second option, the calcium accumulation due to the culture medium contributions was also discarded since both materials were incubated under the same conditions. Therefore, taken into account the cells behaviour in both materials, the calcium detected on the monolayer of cells in the carbon scaffolds could have been produced by osteoblasts.

6. Conclusion

Recent market studies confirmed the global annual growth for the biomaterials sector, due to the aging of the population and to higher social welfare requirements. The pressing need to provide solutions for the replacement, repair and regeneration of tissues and organs brings new challenges. New disciplines such as tissue engineering and regenerative medicine require the convergence of biological sciences, materials engineering and medicine towards the design of scaffolds, with specific morphologies, which will be cultured with cells from the patient *in vitro* to obtain the required living tissue to be implanted. The variability required in the scaffolds properties comes from the specific tissue to engineer and increases the costs of their production. Natural bio-structures offer an enormous potential for the acquisition of microstructures and display the complex and hierarchical organization required in the human organism. The two porous three-dimensional bio-matrices detailed in this chapter aim to provide a promising potential solution for a specific application searched in the bone tissue requirements and focused in the alignment growth by a directional patterning.

7. Acknowledgment

This work was partially financed by POCTEP 0330IBEROMARE1P project, Xunta de Galicia 2010/83 and Ministerio de Ciencia e Innovación (MAT 2010-18281). The technical staff of CACTI (University of Vigo) and Dr. Mariana Landín (University of Santiago de Compostela) are gratefully acknowledged.

8. References

- Abramovitch-Gottlib, L.; Geresh, S. & Vago, R. (2006). Biofabricated marine hydrozoans: A bioactive crystalline material promoting ossification of mesenchymal stem cells. *Tissue Engineering* Vol.12 [4], pp.729-739, ISSN 2152-4947
- Almeida, C.M.R.; Mucha, A. P. & Vasconcelos M.T.S.D. (2006). Variability of metal contents in the sea rush *Juncus maritimus*-estuarine sediment system through one year of plant's life. *Marine Environmental Research*, Vol.61, pp. 424-438, ISSN 0141-1136
- Bettinger, C.J.; Borenstein, J.T. & Langer, R. (2008). Microfabrication techniques in scaffold development, In: *Nanotechnology and tissue engineering. The Scaffold*, C.T. Laurencin & L.S. Nair, (Ed.), 87-113, CRC Press, ISBN 978-1-4200-5182-7 Boca Raton, Florida

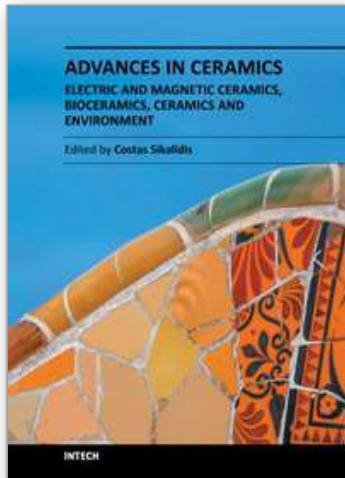
- Borrajo, J.P. (2006). *Cerámicas biomórficas de carburo de silicio recubiertas con materiales bioactivos para aplicaciones biomédicas*. PhD thesis, University of Vigo.
- Byrne, C.E. & Nagle, D.C. (1997). Carbonization of wood for advanced materials applications. *Carbon Journal*, Vol.35, pp. 259-266, ISSN 0008-6223
- Cousins, R.J. (1995). Trace element micronutrients, In: *Molecular biology and biotechnology: a comprehensive desk reference*, R.A. Meyers (Ed.), 899-901, Wiley-Vch, ISBN 0-47118634-1 New York, US
- Cunningham, E.; Dunne, N.; Walker, G.; Maggs, C.; Wilcox, R. & Buchanan, F. (2009). Hydroxyapatite bone substitutes developed via replication of natural marine sponges. *Journal of Materials Science: Materials in Medicine* Article in press, pp. 1-7, ISSN 0957-4530
- Dawes, C.J. (1998). *Marine Botany*, 2nd edition, John Wiley & Sons, ISBN 0-471-19208-2 New York, US
- de Carlos, A.; Borrajo, J.P.; Serra, J.; González, P. & León, B. (2006). Behaviour of MG-63 osteoblast-like cells on wood-based biomorphic SiC ceramics coated with bioactive glass. *Journal of Materials Science: Materials in Medicine*, Vol.17, pp. 523-529, ISSN 0957-4530
- Dragnea, B.; Boulmer, J.; Débarre, D. & Bourguignon, B. (2001). Growth of a SiC layer on Si(100) from absorbed propene by laser melting. *Journal of Applied Physics*, Vol.90, pp. 449-455, ISSN 0021-8979
- Dressler, W. & Riedel, R. (1997). Progress in silicon-based non-oxide structural ceramics. *International Journal of Refractory Metals and Hard Materials*, Vol.15, pp. 13-47, ISSN 0958-0611
- Gómez de Salazar, J.M., Barrena, M.I.; Merino, C.; Plaete, O. & Morales, G. (2007). Preparación y estudio de materiales compuestos nanofibras de carbono/poliéster laminados con fibra de vidrio. *Anales de la Mecánica de Fractura*, Vol.1, pp. 234-238, ISSN 0213-3725
- González, P.; Borrajo, J.P.; Serra, J.; Chiussi, S.; León, B.; Martínez-Fernández, J.; Varela-Feria, F.M.; de Arellano-López, A.R.; de Carlos, A.; Muñoz, F.M.; López, M. & Singh, M. (2009). A new generation of bio-derived ceramic materials for medical applications. *Journal of Biomedical Materials Research Part A*, Vol.88, No.3, pp. 807-813, ISSN 1549-3296
- Green, D.; Howard, D.; Yang, X.; Kelly, M. & Oreffo, R.O.C. (2003). Natural marine sponge fiber skeleton: a biomimetic scaffold for human osteoprogenitor cell attachment, growth and differentiation. *Tissue Engineering* Vol.9, pp. 1159-1166, ISSN 2152-4947
- Green, D.W. (2008). Tissue bionics: examples in biomimetic tissue engineering. *Biomedical Materials* Vol.3, pp.1-11, ISSN 1748-6041
- Harrison, B.S. & Atala, A. (2007). Carbon nanotube applications for tissue engineering. *Biomaterials*, Vol.28, pp. 344-353, ISSN 0142-9612
- Huebsch, N. & Mooney, D.J. (2009). Inspiration and application in the evolution of biomaterials. *Nature* Vol.462, pp. 426-432, ISSN 0028-0836
- Ishizaki, K.; Komarneni, S. & Nanko, M. (1998). *Porous materials: Process technology and application*. Kluwer Academic Publishers, ISBN 0-412-71110-9, Dordrecht, The Netherlands
- Karageorgiou, V. & Kaplan D. (2005). Porosity of 3D biomaterial scaffolds and osteogenesis. *Biomaterials*, Vol.26, pp. 5474-5491, ISSN 0142-9612

- Lakes, R. (1993). Materials with structural hierarchy. *Nature* Vol.361, pp.511-515, ISSN 0028-0836
- López-Álvarez, M.; de Carlos, A.; González, P.; Serra, J. & León, B. (2010). Cytocompatibility of bio-inspired silicon carbide ceramics. *Journal of Biomedical Materials Research Part B Applied Biomaterials*, Vol.95, No.1, pp. 177-183 ISSN 1552-4973
- Maity, A.; Kalita, D.; Kayal, T.K.; Goswami, T.; Chakrabarti, O.; Maiti, H.S. & Rao, P.G. (2010). Synthesis of SiC ceramics from processed cellulosic bio-precursor. *Ceramics International Journal*, Vol.36, pp. 323-331, ISSN 0272-8842
- Pappacena, K.E.; Gentry, S.P.; Wilkes, T.E.; Johnson, M.T.; Xie, S.; Davis, A. & Faber K.T. (2009). Effect of pyrolyzation temperature on wood-derived carbon and silicon carbide. *Journal of the European Ceramic Society*, Vol.29, pp.3069-3077, ISSN 0955-2219
- Qian, J.M. & Jin, Z.H. (2006). Preparation and characterization of porous, biomorphic SiC ceramic with hybrid pore structure. *Journal of the European Ceramic Society*, Vol.26, pp. 1311-1316, ISSN 0955-2219
- Raouf, A. & Seth, A. (2000). Ets transcription factors and targets in osteogenesis. *Oncogene*, Vol.19, pp. 6455-6463, ISSN 0950-9232
- Ratner, B.D. (2004). A history of biomaterials, In: *Biomaterials science: an introduction to materials in medicine*, B.D. Ratner, A. S. Hoffmann and F. J. Schoen, (Ed.), 10-19, Elsevier Academic Press, ISBN 0-12582463-7, London, United Kingdom
- Smith, B. (1999). *Infrared Spectral Interpretation A Systematic Approach*, CRC Press LLC, ISBN 0-84932463-7 Boca Raton, Florida, US
- Singh, M.; Martínez-Fernández, J. & de Arellano-López A.R. (2003). Environmentally conscious ceramics (ecoceramics) from natural wood precursors. *Current Opinion in Solid State & Materials Science*, Vol.7, pp. 247-254, ISSN 1359-0286
- Tang, M.M. & Bacon, R. (1964). Carbonization of cellulose fibers I. Low temperature pyrolysis. *Carbon Journal*, Vol.2, pp.211-214 ISSN 0008-6223
- Varela-Feria, F.M.; de Arellano-López, A.R. & Martínez-Fernández, J. (2002). Fabricación y propiedades del carburo de silicio biomórfico: maderas cerámicas. *Boletín de la Sociedad Española de Cerámica y Vidrio*, Vol.41, pp. 377-384, ISSN 0366-3175
- Wang, J.H.C.; Grood, E.S.; Florer, J. & Wenstrup, R. (2000). Alignment and proliferation of MC3T3-E1 osteoblasts in microgrooved silicone substrata subjected to cyclic stretching., *Journal of Biomechanics* Vol.33, pp. 729-735, ISSN 0021-9290
- Wang, K.; Christensen, K.; Chawla, K.; Xiao, F.; Krebsbach, P.H. & Franceschi, R.T. (1999). Isolation and characterization of MC3T3-E1 preosteoblast subclones with distinct in vitro and in vivo differentiation/mineralization potential. *Journal of Bone and Mineral Research*, Vol.14, pp. 893-903, ISSN 08840431
- Wiemann, M.; Bingmann, D.; Franzka, S.; Hartmann, N.; Urch, H. & Epple, M. (2007). Oriented Growth of Osteoblast-like cells on two-dimensionally structured films of functionalized calcium phosphate nanoparticles on a silicon substrate. *Advanced Engineering Materials* Vol.9 [12], pp.1077-1081, ISSN 1438-1656
- Wise, J.K.; Cho, M.; Zussman, E.; Megaridis, C.M. & Yarin, A.L. (2008). Electrospinning techniques to control deposition and structural alignment of nanofibrous scaffolds for celular orientation and cytoskeletal reorganization, In: *Nanotechnology and Tissue Engineering. The Scaffold*, C.T. Laurencin & L.S. Nair, (Ed.), 243-260, CRC Press, ISBN 978-1-4200-5182-7 Boca Raton, Florida

Yang, F.; Neeley, W.L.; Moore, M.J.; Darp, J.M.; Shukla, A. & Langer, R. (2008). Tissue engineering: the therapeutic strategy of the twenty-first century, In: *Nanotechnology and tissue engineering. The Scaffold*, C.T. Laurencin & L.S. Nair, (Ed.), 3-33, CRC Press, ISBN 978-1-4200-5182-7 Boca Raton, Florida, US

IntechOpen

IntechOpen



**Advances in Ceramics - Electric and Magnetic Ceramics,
Bioceramics, Ceramics and Environment**

Edited by Prof. Costas Sikalidis

ISBN 978-953-307-350-7

Hard cover, 550 pages

Publisher InTech

Published online 06, September, 2011

Published in print edition September, 2011

The current book consists of twenty-four chapters divided into three sections. Section I includes fourteen chapters in electric and magnetic ceramics which deal with modern specific research on dielectrics and their applications, on nanodielectrics, on piezoceramics, on glass ceramics with para-, anti- or ferro-electric active phases, of varistors ceramics and magnetic ceramics. Section II includes seven chapters in bioceramics which include review information and research results/data on biocompatibility, on medical applications of alumina, zirconia, silicon nitride, ZrO₂, bioglass, apatite-wollastonite glass ceramic and b-tri-calcium phosphate. Section III includes three chapters in applications of ceramics in environmental improvement and protection, in water cleaning, in metal bearing wastes stabilization and in utilization of wastes from ceramic industry in concrete and concrete products.

How to reference

In order to correctly reference this scholarly work, feel free to copy and paste the following:

Miriam López-Álvarez, Julia Serra, Alejandro de Carlos and Pío González (2011). Marine-Based Carbon and Silicon Carbide Scaffolds with Patterned Surface for Tissue Engineering Applications, *Advances in Ceramics - Electric and Magnetic Ceramics, Bioceramics, Ceramics and Environment*, Prof. Costas Sikalidis (Ed.), ISBN: 978-953-307-350-7, InTech, Available from: <http://www.intechopen.com/books/advances-in-ceramics-electric-and-magnetic-ceramics-bioceramics-ceramics-and-environment/marine-based-carbon-and-silicon-carbide-scaffolds-with-patterned-surface-for-tissue-engineering-appl>

INTECH
open science | open minds

InTech Europe

University Campus STeP Ri
Slavka Krautzeka 83/A
51000 Rijeka, Croatia
Phone: +385 (51) 770 447
Fax: +385 (51) 686 166
www.intechopen.com

InTech China

Unit 405, Office Block, Hotel Equatorial Shanghai
No.65, Yan An Road (West), Shanghai, 200040, China
中国上海市延安西路65号上海国际贵都大饭店办公楼405单元
Phone: +86-21-62489820
Fax: +86-21-62489821

© 2011 The Author(s). Licensee IntechOpen. This chapter is distributed under the terms of the [Creative Commons Attribution-NonCommercial-ShareAlike-3.0 License](#), which permits use, distribution and reproduction for non-commercial purposes, provided the original is properly cited and derivative works building on this content are distributed under the same license.

IntechOpen

IntechOpen